Journal of Nuclear Materials 392 (2009) 471–475

Contents lists available at ScienceDirect

Journal of Nuclear Materials

journal homepage: www.elsevier.com/locate/jnucmat

Synthesis and characterization of Li_4SiO_4 nano-powders by a water-based sol–gel process

Xiangwei Wu, Zhaoyin Wen *, Xiaogang Xu, Xiuyan Wang, Jiu Lin

Shanghai Institute of Ceramics, Chinese Academy of Sciences, 1295 Dingxi Road, Shanghai 200050, PR China

ARTICLE INFO

Article history:
Received 30 October 2008
Accepted 13 April 2009

ABSTRACT

The water-based sol–gel process for the synthesis of Li_4SiO_4 nano-powders was reported for the first time. $LiOH{\cdot}H_2O$ and aerosil SiO_2 were used as the starting materials with citric acid ($C_6H_8O_7{\cdot}H_2O$) as the chelating agent. Li_4SiO_4 powders with particle size as small as 100 nm were successfully synthesized at the temperature as low as 675 °C. Phase analysis, morphology, sintering behavior of the powders and ionic conductivity of the sintered bodies were investigated systematically. The experimental results showed that the powders obtained by the water-based sol–gel process (SG) possessed excellent sinterability, exhibiting a linear shrinkage of 5.2% while sintered to 900 °C, more than 3 times that of the powders obtained by solid state reaction (SSR). The bulk conductivity of the SG sintered bodies was much higher than that of the SSR samples at the same testing temperature.

© 2009 Elsevier B.V. All rights reserved.

1. Introduction

Lithium orthosilicate (Li_4SiO_4) and its solid solution are known as fast Li-ion conductors [1,2]. As a CO_2 catalytic/sorbent, Li_4SiO_4 also exhibits excellent performance [3]. Recently, Li_4SiO_4 has been selected as one of the most promising candidates for solid tritium breeding materials in fusion reactors because of its high lithium atom density and favorable tritium release behaviors [4–6]. For the breeding materials, the migration behavior of tritium in breeders is an important item, which was significantly related to the Li-ion conductivity [7]. The ionic conductivity of ceramics is affected by the synthetic method.

In previous studies, several methods are available for synthesis of Li_4SiO_4 powders. Traditional solid state reaction or precipitation methods require high temperature (usually $\geqslant$900 °C) and lead to many problems including volatilization and lack of control of the microstructure and composition [8,9]. The combustion method could hardly produce pure Li_4SiO_4 because of the deficiency of oxygen or the formation of Li_2CO_3 [10,11]. A method, using $LiOH{\cdot}H_2O$/$LiNO_3$ and fumed silica as the starting materials, was reported to fabricate microsize Li_4SiO_4 powders [8]. The sol–gel method is a preferred choice to synthesize ceramic powders, since it offers an opportunity for not only synthesizing a material at low temperatures but also the possibility to control its morphology and microstructure. The sol–gel methods based on alkoxide precursors or using tetraethyl orthosilicate (TEOS) and $LiOH{\cdot}H_2O$ as the starting materials were performed to synthesize Li_4SiO_4 nano-powders [9,12]. However, these sol–gel processes were all carried out in organic medium.

The aim of the present work was to develop a water-based sol–gel route to synthesize Li_4SiO_4 nano-powders, which was low cost and easy to control. SiO_2 (aerosil) and $LiOH{\cdot}H_2O$ were used as the starting materials with citric acid ($C_6H_8O_7{\cdot}H_2O$) as the chelating agent. Li_4SiO_4 powders with primary particle size as small as 100 nm were successfully synthesized at 675 °C, which was much lower than the solid state reaction method ($\geqslant$900 °C). The sinterability of the obtained Li_4SiO_4 powders and the Li-ion conductivity of the Li_4SiO_4 ceramics were investigated.

2. Experimental procedure

2.1. Preparation of Li_4SiO_4 powders

Li_4SiO_4 powders were prepared by solid state reaction and the water-based sol–gel method, respectively. In the synthesis by solid state reaction, the powders of SiO_2 (Analytical Reagent, AR) and Li_2CO_3 (AR) were blended with the Li/Si molar ratio of 4 by planetary ball milling for 4 h using ethyl alcohol as the milling medium. Li_4SiO_4 powders were obtained by calcining the dried precursors at 900 °C for 4 h. For the water-based sol–gel method, SiO_2 (aerosil) and $LiOH{\cdot}H_2O$ (AR) were chosen as the starting materials with citric acid ($C_6H_8O_7$) as the chelating agent. The detailed procedure for the preparation process is shown in Fig. 1. $LiOH{\cdot}H_2O$ was dissolved in distilled water. $C_6H_8O_7$ was used to adjust the pH value of the solution to 8.5. The concentration of lithium ion in the solution was controlled at about 0.3 mol/L. Stoichiometric aerosil SiO_2 was added into the solution and colloidal solution was then obtained. The colloidal solution was vaporized at 70 °C and a

---

* Corresponding author. Tel.: +86 21 52411704; fax: +86 21 52413903.
E-mail address: zywen@mail.sic.ac.cn (Z. Wen).

0022-3115/$ - see front matter © 2009 Elsevier B.V. All rights reserved.
doi:10.1016/j.jnucmat.2009.04.010

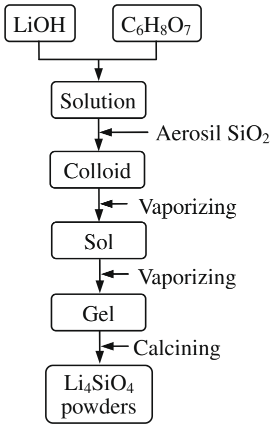

Fig. 1. The sol–gel procedure for the preparation of Li_4SiO_4 powders.

transparent gel was formed ultimately. The gel was dried at 150 °C for 24 h. The dried precursor was sieved with 200 mesh screen and then calcined at 675 °C for 4 h.

2.2. Characterization techniques

Thermal behavior of the gel-precursor was analyzed by thermogravimetry and differential scanning calorimetry (TG/DSC) (NETZSCH STA 409 PC) in air at a constant heating rate of 10 °C/min in the temperature range between room temperature (RT) and 900 °C. Phase analysis was conducted by X-ray diffraction (Rigaku RAD-C, 12KW) at room temperature using CuKα radiation. The morphology of the powders was observed by the field emission scanning electron microscopy (FESEM, JSM-6700F). The linear thermal shrinkage behavior of the Li_4SiO_4 ceramics was evaluated using a dilatometer (NETZSCH DIL 402 C) in the temperature range of 200–1000 °C at a constant heating rate of 5 °C/min in air. The microstructure of the fracture surface of the sintered pellets was observed by scanning electron microscopy (EPMA-8705QH$_2$). The AC impedance spectroscopy measurements were carried out by impedance analyzer (SOLARTRON 1260) with platinum as the blocking electrode in the temperature range of 250–400 °C and the frequency range of 0.1–10^6 Hz.

3. Results and discussion

3.1. Thermal behavior of the gel and phase evolution

The gel precursors for the preparation of the Li_4SiO_4 powders were characterized by TG/DSC to determine the crystallization temperature. Fig. 2 reveals the typical TG/DSC profiles of the gel precursors during the thermal treatment process. Phase evolution of the gel during the thermal treatment was also investigated. Fig. 3 presents the XRD diffractograms of the precursors treated at each temperature corresponding to the thermal events in DSC curve. As seen from Fig. 3, the main phase of the products was Li_2CO_3 when the precursors were calcined at 280 °C for 4 h. In DSC curve, a weak exothermic peak was found at 280 °C, which was associated with the carbonization of the gel and the formation of Li_2CO_3. The main chemical reaction in this process was as follows:

$$2[Li(H_2O)x]OH + CO_2 \rightarrow Li_2CO_3 + (2x+1)H_2O \uparrow . \quad (1)$$

The decomposition of the metal citrate gave rise to the exothermic peak at 368 °C in DSC curve and the diffraction peaks of Li_2CO_3 were detected on the XRD patterns correspondingly. The corresponding chemical reaction was:

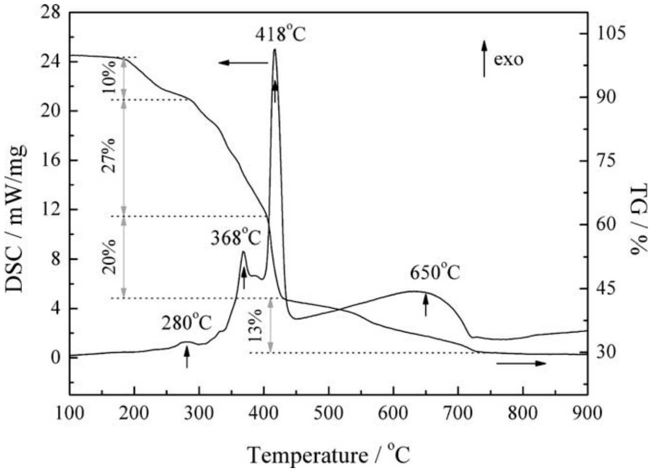

Fig. 2. DSC/TG analysis results of the gel precursors.

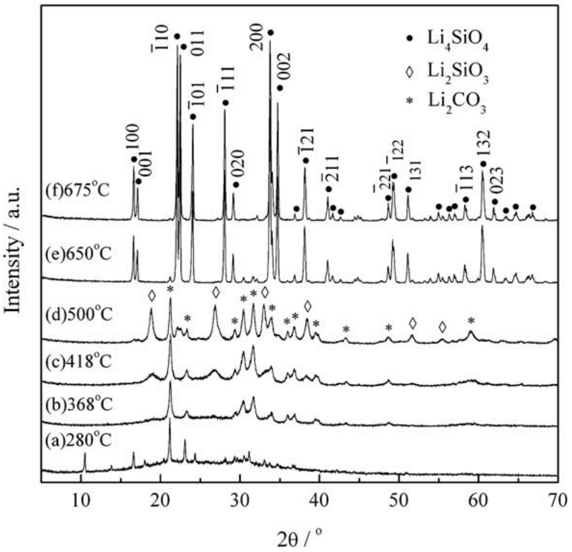

Fig. 3. XRD patterns of the gel precursors treated at different temperatures.

$$2Li_2C_6H_6O_7 + 9O_2 \rightarrow 2Li_2CO_3 + 10CO_2 \uparrow + 6H_2O \uparrow . \quad (2)$$

A new phase, Li_2SiO_3, was obtained after the gel-precursor calcined at 418 or 500 °C according to the XRD analytic results. Therefore, the significant exothermic peak at 418 °C in DSC curve could be attributed to the formation of Li_2SiO_3. The following chemical reaction was suggested for this process:

$$Li_2CO_3 + SiO_2 \rightarrow Li_2SiO_3 + CO_2 \uparrow . \quad (3)$$

While sintered at 650 °C, sharp diffraction peaks corresponding to Li_4SiO_4 (JCPDS 37-1472) were observed in the XRD diffractograms. Li_2CO_3 was also observed on the XRD patterns, however, the intensity of the peaks became very weak, indicating low content of Li_2CO_3 in the products. The broad peak at 650 °C in DSC curve could be explained as the exothermic effects of the formation of Li_4SiO_4:

$$Li_2SiO_3 + Li_2CO_3 \rightarrow Li_4SiO_4 + CO_2 \uparrow , \quad (4)$$

$$2Li_2CO_3 + SiO_2 \rightarrow Li_4SiO_4 + 2CO_2 \uparrow . \quad (5)$$

Further increasing the calcining temperature to 675 °C, the diffraction peaks of Li_2CO_3 were disappeared and only sharp diffraction peaks of Li_4SiO_4 were seen in the XRD diffractograms, demonstrating pure Li_4SiO_4 was synthesized by the water-based sol–gel method at the temperature as low as 675 °C.

3.2. Microstructure of the Li_4SiO_4 powders

The morphology of Li_4SiO_4 powders synthesized by solid state reaction and sol–gel method was observed. In Fig. 4, the SEM images of the Li_4SiO_4 powders prepared by different methods are exhibited. As seen, the samples obtained by solid state reaction (900 °C 4 h) show irregular grains. The grain size had a wide distribution, mainly ranging from 10 to 20 μm with a few grains as large as 30 μm (Fig. 4(a)). The samples prepared by the water-based sol–gel method (675 °C 4 h) displayed different morphology. The grains were spherical and the grain size had a homogeneous distribution (Fig. 4(b)). The average grain size was about 100 nm, which was much smaller than that of the samples obtained by solid state reaction. Compared to the solid state reaction procedure, the reactants were mixed more homogeneously in the sol–gel process because of the liquid–liquid contact and the faster reaction rate, which might explain the morphological differences between the Li_4SiO_4 powders synthesized by the two methods.

3.3. Sintering behavior of the Li_4SiO_4 powders

The as-synthesized powders by solid state reaction (SSR) at 900 °C for 4 h and the water-based sol–gel (SG) process at 675 °C for 4 h were pressed into Li_4SiO_4 bar with size of $\phi 5 \times 25$ mm under 2 MPa pressure, respectively. Fig. 5 shows the thermal shrinkage curve versus temperature. As observed from the dilatometric curve, a slight thermal dilation was found below 640 °C and a rapid decrease of the length was occurred above 640 °C for both the SSR bar and the SG bar. Subsequently, the thermal shrinkage processes completed at 860 °C for the SSR bar and at 915 °C for the SG bar. The linear shrinkage of the SG bar was about 5.2%, more than 3 times that of the SSR bar, indicating much higher sinterability of the Li_4SiO_4 powders obtained by the water-based sol–gel method. The higher sinterability was attributed to the smaller particle size and higher specific surface area of the powders. The high sinterability was beneficial to obtain dense Li_4SiO_4 ceramics, which was an important aspect of the tritium breeding materials.

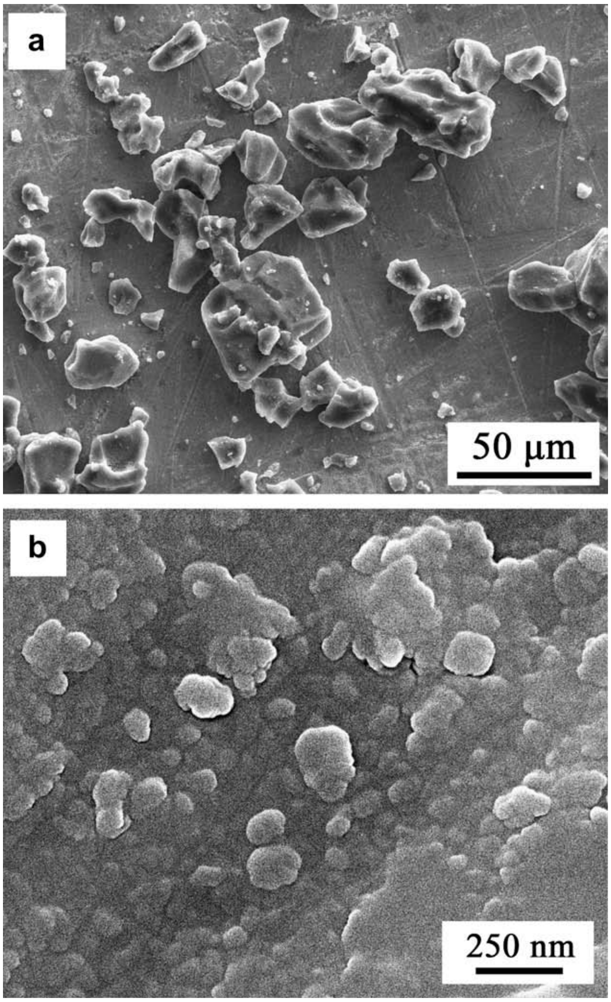

Fig. 4. SEM images of the Li_4SiO_4 powders synthesized by (a) solid state reaction and (b) the water-based sol–gel method.

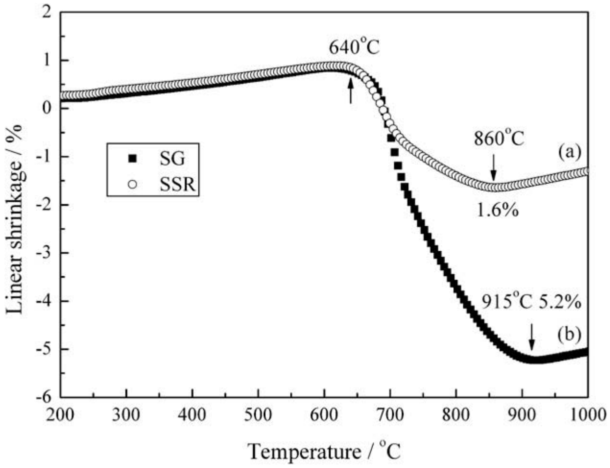

Fig. 5. Thermal shrinkage behaviors of Li_4SiO_4 powders fabricated by (a) solid state reaction and (b) the water-based sol–gel method.

3.4. Ionic conductivity of the Li_4SiO_4 sintered bodies

Li_4SiO_4 powders were synthesized by solid state reaction (900 °C 4 h) and the water-based sol–gel method (675 °C 4 h), respectively. The synthesized Li_4SiO_4 powders were pressed into pellets with 10 mm in diameter under 4 MPa pressure. The green bodies were further iso-statically pressed under 200 MPa. Sintered pellets were then obtained by heating the green bodies at 1000 °C for 4 h. The pellets fabricated from the powders prepared by solid state reaction and the water-based sol–gel process, were marked as SSR and SG samples, respectively. The size and the density of the sintered pellets are shown in Table 1. It was observed from Table 1 that the SSR pellets and the SG pellets were both shrunk after sintered. For the SG pellets, the shrinkage in the radial direction was much larger and the sintered density was much higher, which resulted from the higher sinterability of the SG powders (Fig. 5). The microstructure of the fracture surface of the pellets is presented in Fig. 6. As shown in Fig. 6, the SG pellets displayed homogeneous microstructure and the grain size had a narrow distribution in 5–10 μm. Whereas, the interior of the SSR pellets was heterogeneous and some grains grew as large as 20 μm.

The typical Cole–Cole–Diagram measured at 300 °C for the SSR and SG samples are shown in Fig. 7(a). A high frequency semicircle

Table 1
The size and the density of the sintered Li_4SiO_4 pellets.

Sample	Diameter (ϕ/mm)	Thickness (d/mm)	Relative density (%TD)[a]
SSR	9.78	2.00	77.5
SG	9.58	1.96	82.9

[a] The theoretical density (TD) of Li_4SiO_4 is 2.40 g/cm^3 [4].

follower by the low frequency spike was observed in the plots. According to Bauerle's theory, the left and the right intercepts of the semicircle with the real axis corresponded to the grain interior resistance and the bulk resistance (grain interior resistance plus grain boundary resistance), respectively, and the low frequency spike represented the polarization resistance of the sample-electrode interface [13]. The equivalent circuit was composed of a resistance R1 in series with a component consisting of another resistance R2 in parallel to a CPE element. As seen from Fig. 7(a), the grain interior resistance was comparable for SSR and SG samples, but the bulk resistance was much lower for the SG samples.

The conductivity values of the bulk conductivity (σ_b) can be calculated with $\sigma_b = d/SR_b$, where d is the sample thickness, S, the area of the electrode and R_b, the bulk resistance. The values of these parameters are listed in Table 2. The temperature dependence of the bulk conductivity is illustrated in Fig. 7(b). The conductivity data are found to be linear and well fit the Arrhenius equation, $\sigma_b T = A\exp(-E_\alpha/kT)$, where A is the pre-exponential factor, E_α the activation energy for conduction and k the gas constant, demonstrating that there is no structure and phase change for the samples in the testing temperature range. The bulk conductivity enhanced significantly with the increase of temperature. At 400 °C, the bulk conductivity for the SG samples was about 1.0×10^{-3} S cm^{-1}, nearly 2 orders of magnitude higher than that of the value at 250 °C (1.40×10^{-5} S cm^{-1}). At the same testing temperature, the SG samples possessed much higher bulk conductivity. For example, at 300 °C, the ionic conductivity for the SG samples was 8.27×10^{-5} S cm^{-1}, nearly 1.5 times that of the SSR samples (5.82×10^{-5} Scm^{-1}).

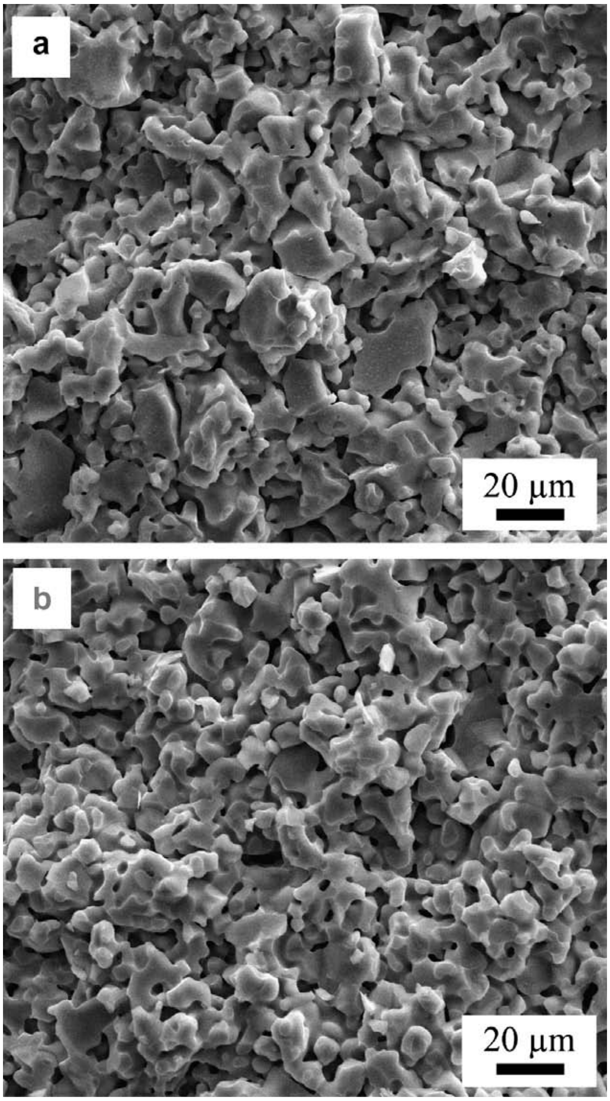

Fig. 6. The microstructure of the cross section of Li_4SiO_4 pellets: (a) SSR samples and (b) SG samples.

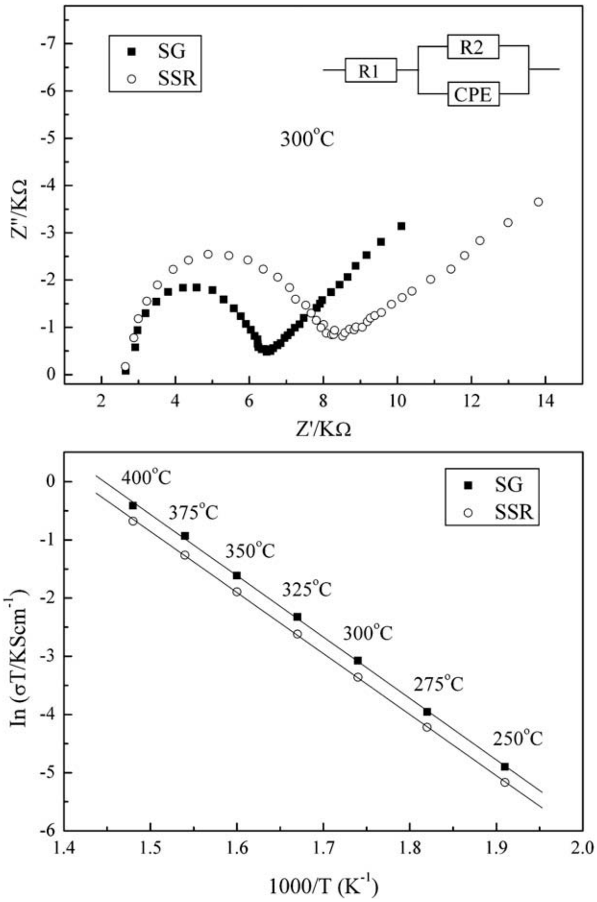

Fig. 7. (a) Cole–Cole–Diagram of Li_4SiO_4 ceramics at 300 °C, (b) Arrhenius plots of the bulk conductivity for the Li_4SiO_4 samples.

The activation energy E_α, on the other hand, made no difference for both the SSR and the SG samples, being about 87.6 and 87.2 kJ/mol, respectively, indicating the same conduction mechanism for the SSR and the SG samples. As the grain conductivity was almost equal at the same testing temperature, the improvement of the ionic conductivity for the SG samples was ascribed to the enhancement of the grain boundary conductivity. For the SG samples, the grain boundary increased because of the smaller particle size and more homogeneous structure (Fig. 6(b)), which provided more paths for ion conductivity and thus resulted in the enhancement of the bulk conductivity. The improved sintered density of SG samples (Table 1) was also beneficial to the enhancement of the bulk conductivity.

Table 2
The value of sample thickness, area of electrode, and the bulk resistance.

Sample	Thickness (d/mm)	Area of electrode (S/mm^2)	Bulk resistance (300 °C) (R_b/Ω)
SSR	1.18	23.6	8588.4
SG	1.18	23	6204.1

4. Conclusions

Li_4SiO_4 nano-powders with primary particle size of about 100 nm were synthesized by a newly developed sol–gel method using water as the reaction medium and $LiOH{\cdot}H_2O$ and aerosil SiO_2 as the starting materials at the temperature as low as 675 °C. The obtained Li_4SiO_4 powders exhibited excellent sinterability due to the small particle size and high specific surface area. Compared to the SSR samples, the SG samples possessed much higher ionic conductivity because of the more homogeneous structure and higher density of the SG samples at the same testing temperature. At 400 °C, the bulk conductivity for the SG samples was as high as 1.0×10^{-3} S cm^{-1}.

Acknowledgements

The authors would like to thank Professor Jianguo Wu in Tongji University and Mr Xiaohe Xu in Shanghai Institute of Ceramics, Chinese Academy of Sciences, for their assistance throughout the experimental work of this research.

References

[1] A.D. Robertson, A.R. West, A.G. Ritchie, Solid State Ionics 104 (1997) 1.
[2] A. Khorassani, A.R. West, Solid State Ionics 7 (1982) 1.
[3] M. Kato, in: Proceedings of the Sixth Workshop on the International Test Network for CO_2 Capture, Trondheim, 2004.
[4] G. Piazza, J. Reimann, E. Günther, R. Knitter, N. Roux, J.D. Lulewicz, J. Nucl. Mater. 307&311 (2002) 811.
[5] L.V. Boccaccini, L. Giancarli, G. Janeschitz, S. Hermsmeyer, Y. Poitevin, A. Cardella, E. Diegele, J. Nucl. Mater. 329&333 (2004) 48.
[6] H. Werle, W. Breitung, M. Briec, R.G. Clemmer, H. Elbel, H.E. Häfner, M. Masson, G. Schumacher, H. Wedemeyer, J. Nucl. Mater. 155&157 (1988) 538.
[7] H. Ohno, S. Konishi, T. Nagasaki, T. Kurasawa, H. Katsuta, H. Watanabe, J. Nucl. Mater. 133&134 (1985) 181.
[8] C.C. Chang, C.C. Wang, P.N. Kumta, Mater. Design 22 (2001) 617.
[9] H. Pfeiffer, P. Bosch, S. Bulbulian, J. Nucl. Mater. 257 (1998) 309.
[10] D. Cruz, S. Bulbulian, J. Nucl. Mater. 312 (2003) 262.
[11] D. Cruz, S. Bulbulian, J. Am. Ceram. Soc. 88 (2005) 1720.
[12] M. Smaihi, J.P. Boilot, P. Bergez, M.J. Boncoeur, in: G.W. Hollenberg, I.J. Hastings (Eds.), Fabrication and Properties of Lithium Ceramics II, Advances in Ceramics, vol. 27, The American Ceramic Society, Westerville, OH, 1990, p. 35.
[13] J.E. Bauerle, J. Phys. Chem. Solids 30 (1969) 2657.